

Full Paper

Detection of Clindamycin in Pharmaceutical Products using an Electrochemiluminescence Electrode based on a Composite of Ru(bpy)₃²⁺, Eu₂O₃ Nanoparticle and Chitosan

Sepideh Mohammad Beigi,¹ Fazeleh Mesgari,¹ and Morteza Hosseini^{2,*}

¹*Center of Excellence in Electrochemistry, School of Chemistry, College of Science, University of Tehran, Tehran, Iran*

²*Department of Life Science Engineering, Faculty of New Sciences & Technologies, University of Tehran, Tehran, Iran*

*Corresponding Author, Tel.: +982186093196

E-Mail: hosseini_m@ut.ac.ir

Received: 5 March 2020 / Received in revised form: 23 April 2020 /

Accepted: 28 April 2020 / Published online: 31 May 2020

Abstract- In this study, the electrochemiluminescence (ECL) interaction of clindamycin and tris(2,2'-bipyridine)ruthenium(II) (Ru(bpy)₃²⁺) was used to develop a sensitive tool for the detection of clindamycin based on modifying a glassy carbon electrode (GCE) with nanoparticles of europium oxide. The experiments showed that in the presence of these inorganic nanoparticles (Eu₂O₃ NPs) the ECL signal is enhanced. The optimal ECL response of the electrode was found to linearly change with the concentration of clindamycin from 3.0×10⁻¹⁴ to 1.0×10⁻⁶ mol L⁻¹ (R²= 0.9909) and a detection limit of as low as 7.4×10⁻¹⁵ mol L⁻¹ (S/N=3) with a relative standard deviation (RSD) of 4.0 % was observed. The method was compared and found to be better than previously reported ones, in terms of sensitivity, and the analysis of the analyte by proposed method was successful in pharmaceutical formulations using HPLC as a reference method.

Keywords- Electrochemiluminescence; Clindamycin; Europium oxide; Antibiotic

1. INTRODUCTION

Clindamycin (Fig. 1) is a lincosamide antibiotic used for treating humans and animals [1]. The compound is usually used for treating acne, malaria, bacterial vaginal, streptococcal, staphylococcal infections as well as an antimicrobial agent. The side effects of clindamycin include skin dryness, burning, itching, peeling, and rash, nausea, vomiting, and constipation. There are also concerns about the bacterial resistance to clindamycin due to excessive use [2, 3].

Some of the methods used for the analysis of clindamycin include chemiluminescence [4], spectrophotometry [5], micelle are lectrokinetic chromatography [1], high-performance liquid chromatography [6-8], stripping voltammetry [9], and capillary electrophoresis [10, 11]. Most of the mentioned methods are time intensive and require complex operation and special sample pre-treatments and also present lower sensitivity required for different biological and environmental samples, and hence there is always a need for another development of alternative techniques for this end.

ECL is the phenomenon observed at electrode surfaces, according to which excited species emit light [12-16]. This phenomena has changed to an attractive and powerful mechanism for building biosensors and bioassays, due to its high sensitivity and electivity, low background, wide linear range, and the low costs of the required equipment [17-19].

The $\text{Ru}(\text{bpy})_3^{2+}$ system has found widespread applications in the analysis of amino acids [20], drugs [21-23], DNA [24,25] and proteins [26-28], due to its excellent stability, high ECL quantum yield and biocompatibility. Reports have stated that immobilizing $\text{Ru}(\text{bpy})_3^{2+}$ on the electrode surface could be used as a strategy for decreasing consumption of expensive reagents, and enhancement of the ECL signals using simple designs [29].

On the other hand, rather recently there has been an incremental trend in the area of the application of nanomaterials, such as graphene and carbon nanostructures in order to enhance the surface qualities of electrode [30-38]. As an example using metal nanoparticles to this end, has been found to create distinct advantages like better mass transport and lower dependency to the solution resistance, as well as enhanced limits of detection and signal/noise ratios [39-44].

More specifically rare earth elements due to their unique chemical properties have been subject to a wide range of research [45-49]. Rare earth oxides (REOs) as promising compounds are applied for optoelectronic devices, logical switches, and memories [50] due to their considerable mechanical stability and dielectric constants, as well as large band gap values. REOs are also well known due to their high surface basicity, fast oxygen ion mobility and unique catalytic behaviours [51].

Nanoparticles of Eu_2O_3 , as an instance, are one of the most promising materials for application in bio application, low voltage and cathode based devices up-conversion materials, supercapacitors, electro-analytical and photo-electrochemical based devices [52-

56]. The interesting chemical and electrochemical behaviours of Eu_2O_3 nanoparticles such as electrocatalytic property and electron mediation originated from their 4f electron configuration [57-59].

Accordingly, this work was focused on the application of Eu_2O_3 NPs to modify a glassy carbon electrode (GCE) and act as a mediator between the surface of the GCE and the incorporated $\text{Ru}(\text{bpy})_3^{2+}$. The intention was to increase the oxidation currents of $\text{Ru}(\text{bpy})_3^{2+}$ and hence forge a very sensitive ECL sensor for clindamycin.

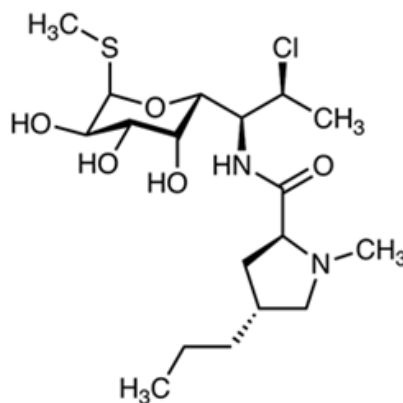


Fig. 1. The chemical structure of clindamycin

2. EXPERIMENTAL

2.1. Reagents and chemicals

Analytical reagent grade chemical materials were obtained from the suppliers and used without further purification. Tris(2,2'-bipyridyl) ruthenium(II) ($\text{Ru}(\text{bpy})_3^{2+}$) chloride hexahydrate was supplied by Sigma-Aldrich. The phosphate buffer solution (PBS, $\text{pH}=7.5$) was prepared through mixing proper amounts of K_2HPO_4 , NaH_2PO_4 , and KCl followed by adjusting the pH .

2.2. Apparatus

The electrochemical set-up included a three-electrode system composed of a Pt wire (auxiliary electrode), an $\text{Ag}|\text{AgCl}|\text{KCl}$ sat'ed reference electrode and the developed sensor as the working electrode. The cyclic voltammetry (CV) experiments were conducted on a Palm Sens PC potentiostat-galvanostat. The Eu_2O_3 NP/ $\text{Ru}(\text{bpy})_3^{2+}$ /GCE working electrode was equatorially mounted onto a 4mL quartz cell, located in front of ECL detector (a Perkin-Elmer LS 50 photomultiplier.) and all ELC tests were run in a light tight black box.

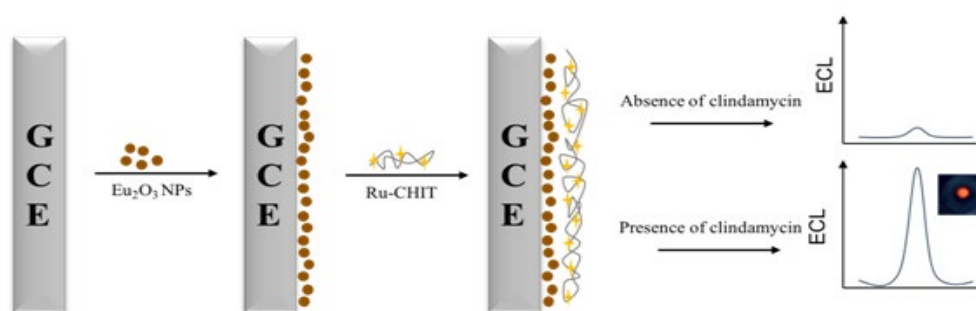
The morphology of the $\text{Eu}_2\text{O}_3\text{NP}/\text{Ru}(\text{bpy})_3^{2+}/\text{GCE}$ was studied using a KYKY-EM 3200 digital scanning electron microscope and the size of the Eu_2O_3 NPs was evaluated by scanning electron microscopy (SEM) analyses.

2.3. Synthesis of Eu₂O₃NPs

According to former reports on lanthanide oxide NPs [21-22], the process started with dissolving europium oxide powder in a proper concentration of HNO₃ through ultrasonication and following diluted with ethanol. Next, polyvinyl alcohol (PVA) and water mixture (20:80 wt%) were added to this solution while it was vigorously stirred. As a next step, 2 ml of a 32% aqueous ammonium hydroxide solution in a dropwise manner, was added to the resulting mixture, and then was heated to 90 °C while stirring for 2 hours. The dense porous gel formed after the stages, was the product of the condensation of the hydroxyl network and was dedicated at 110 °C in an oven. The dry product was eventually calcinated at 400 °C to yield Eu₂O₃ NPs.

2.4. Preparing the sensor

The first step to prepare the sensor was preparing the surface of the glassy carbon electrode. To this end for polishing cloth, a GCE was polished using 1.0, 0.3, and 0.05 μm alumina slurries, and then washed thoroughly with water, and further cleaned by sonication in ethanol and water. Next 100 μL of a 2.5 × 10⁻³ mol L⁻¹ Ru(bpy)₃²⁺ solution in water, was added to 600 μL of a 0.5 wt% suspension of chitosan (the chitosan suspension was prepared by addition of 50.0 mg of the compound in 10.0 mL of 3% acetic acid). The Eu₂O₃ NPs/Ru(bpy)₃²⁺/CHIT electrode was finally prepared by casting 12 μl of a suspension of Eu₂O₃ on the surface of the electrode, and drying the resulting assembly under ambient conditions, followed by adding 6 μl of the above-mentioned Ru(bpy)₃²⁺/CHIT suspension onto the surface of Eu₂O₃ NPs/GCE at room temperature (Scheme 1).



Scheme 1. Schematic representation of the fabrication of ECL sensor

2.5. The pharmaceutical samples

The pharmaceutical samples were obtained from the local market and then treated to be ready for the analyses. This included accurately weighing a total of 10 clindamycin tablets one by one. Then the tablets were mixed and a specific amount of clindamycin (equivalent to 1 tablet or caplet), was taken and weighted. This sample was dissolved in 100 mL flask

containing water under sonication and then further diluted to reach the concentration within the calibration range of the sensor. The results were checked with those obtained through HPLC, as a reference method.

3. RESULTS AND DISCUSSION

3.1. Characterization of the Eu_2O_3 NPs

The structural properties of the Eu_2O_3 NPs were evaluated by SEM and the results are given in Fig. 2. As it can be seen, the Eu_2O_3 NPs have a narrow size distribution, and the uniform modification of the surface of the modified GCE.

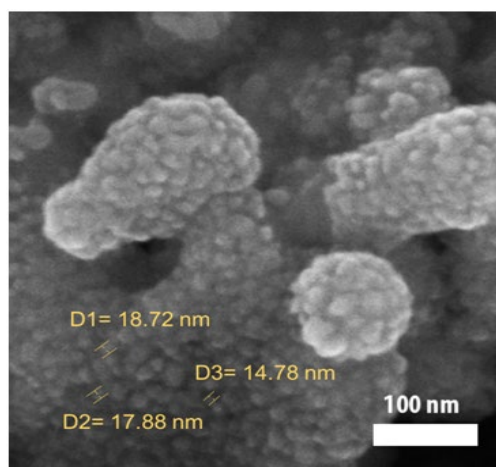


Fig. 2. SEM image of Eu_2O_3 NPs

3.2. Electrochemical and ECL performances of the Eu_2O_3 NPs/ $\text{Ru}(\text{bpy})_3^{2+}$ /GCE

Electrochemical impedance spectroscopy (EIS), as one of the most informative electrochemical methods, was used for characterization of the surface modification process of the electrochemical sensor. As shown in Fig. 3, the Nyquist plots at different modified states. The electron-transfer-limited process and the diffusion process resulted to semicircular portion and the linear portion of the impedance spectra, respectively. The observed semicircle diameters correspond to the electron-transfer resistance (R_{et}). Chitosan as a kind of insulating polymer, caused inhibition in the electron-transfer at the electrode surface, thus resulted to increase in R_{et} was because of the modification of chitosan (curve b). After modification of the electrode with Eu_2O_3 NPs, the diameter of semicircle was much smaller, demonstrating a lower R_{et} value for $[\text{Fe}(\text{CN})_6]^{3-/4-}$ (curve c). This observation confirmed that the Eu_2O_3 NPs increased the surface conductivity of the electrode.

The effects of pure metal and metal oxide NPs, e.g. Sm_2O_3 [21] and CeO_2 [26,27] on ECL properties have been formerly evaluated. In the case of the Eu_2O_3 NP/GCE these behaviours were studied through recording CVs at a scan rate of 100 mV s^{-1} , in the potential window of

0.0 to 1.8 V (vs. Ag|AgCl|KCl_{sat}). The CVs obtained using GCE, GCE/Ru(bpy)₃²⁺ and Eu₂O₃ NP/Ru(bpy)₃²⁺/GCE in a PBS (pH=7.5) are presented in Fig. 4. Clearly Eu₂O₃ NP/Ru(bpy)₃²⁺/GCE produce larger charging currents due, most probably, to their higher surface area, as well as the facilitated electron mediation between Ru(bpy)₃²⁺ and the glassy carbon, due to the presence of the Eu₂O₃ NPs. In the case of the modified electrode a further couple of redox peaks could be observed at +0.97.

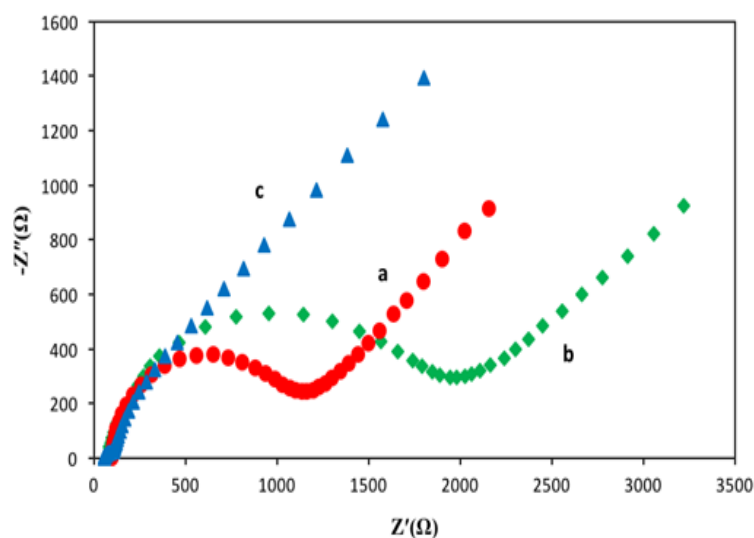


Fig. 3. Nyquist impedance spectra of (a) GCE, (b) Ru(bpy)₃²⁺/chitosan/GCE, (c) Eu₂O₃/Ru(bpy)₃²⁺/chitosan/GCE, solution containing [Fe(CN)₆]^{4-/3-} 5 mM and KCl 250 mM

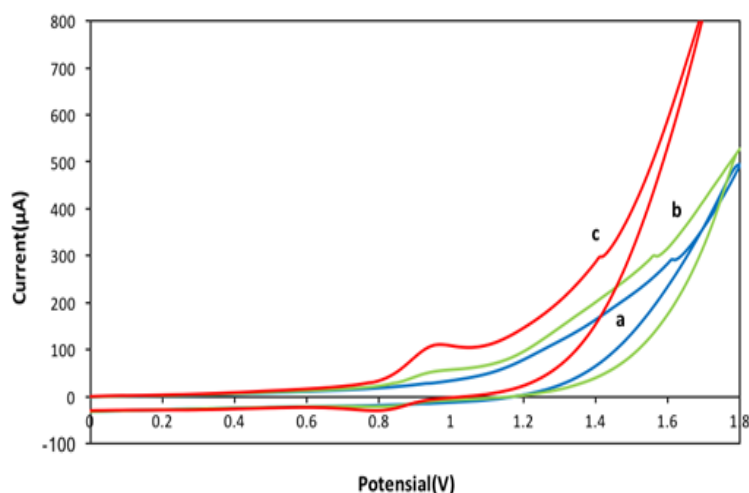


Fig. 4. Cyclic voltammograms GCE (a), Ru(bpy)₃²⁺-GCE (b), Eu₂O₃ NPs-Ru(bpy)₃²⁺- GCE (c); supporting electrolyte buffer solution (0.1mol L⁻¹ and pH 7.5) and 5×10⁻⁸ mol L⁻¹ Clindamycin; potential scan rate, 100 mV s⁻¹

The presence of Eu_2O_3 NPs in the GCE composition was found to increase the ECL signal (Fig. 5). This seems to be the effect of the improved oxidation of $\text{Ru}(\text{bpy})_3^{2+}$ in the presence of these inorganic nanoparticles, leading to increases in the electro-generated CL species and hence the better sensitivity.

To optimize the ECL response of the sensor to clindamycin the effects of pH, $\text{Ru}(\text{bpy})_3^{2+}$ concentration and the scan rate were assessed and optimized.

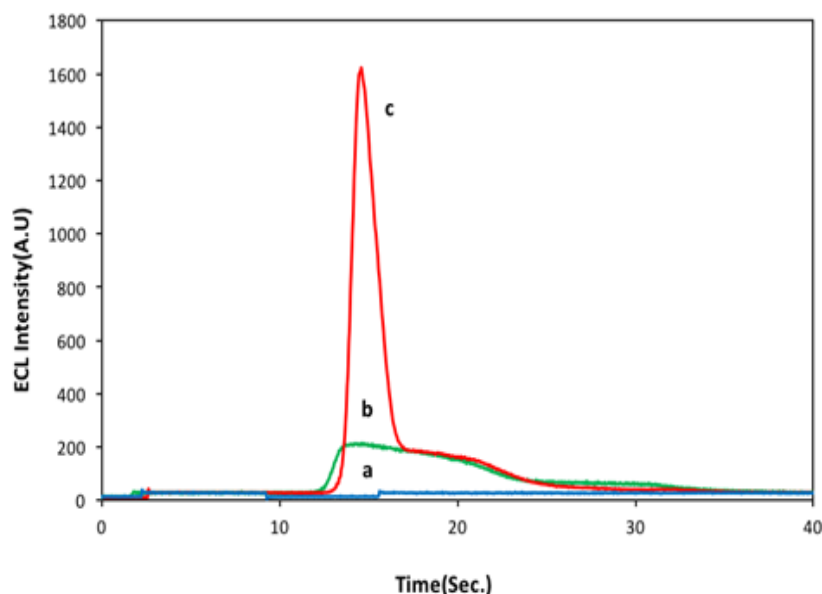


Fig. 5. ECL responses of GCE (a), $\text{Ru}(\text{bpy})_3^{2+}$ -GCE (b), Eu_2O_3 NPs- $\text{Ru}(\text{bpy})_3^{2+}$ -GCE (c) in 0.1 mol L^{-1} pH 7.5 phosphate buffer containing $5 \times 10^{-8} \text{ mol L}^{-1}$ Clindamycin; potential scan rate, 100 mV s^{-1}

3.3. Effect of pH

The effect of pH on the ECL signal of the analyte was evaluated in a range of 5.5-9.5 and based on the results (Fig. 6a), it was found that the ECL intensity considerably increased as a function of pH from 5.5 to 7.5, yet it dropped at pH values over 7.5. As a result 7.5 was chosen as the optimal pH, and that of the PBS used was adjusted at this value.

3.4. Effect of $\text{Ru}(\text{bpy})_3^{2+}$ concentration

Studies on the effect of the $\text{Ru}(\text{bpy})_3^{2+}$ concentration in the GCE on the ECL signal was studied using a $5 \times 10^{-8} \text{ mol L}^{-1}$ clindamycin solution. The observations indicated that the intensity of the ECL signal linearly increased with increasing $\text{Ru}(\text{bpy})_3^{2+}$ concentration from 1.0×10^{-2} to $2.5 \times 10^{-3} \text{ mol L}^{-1}$ and remained almost constant above this range. On the other hand the background ECL signal of $\text{Ru}(\text{bpy})_3^{2+}$ steadily increased in the same range and hence $2.5 \times 10^{-3} \text{ mol L}^{-1}$ was concluded as the optimal value for $\text{Ru}(\text{bpy})_3^{2+}$ concentration for

obtaining the best ECL response using the Eu_2O_3 NP/ $\text{Ru}(\text{bpy})_3^{2+}$ /GCE in the determination of clindamycin.

3.5. Effect of scan rate

To monitor the behaviour of the ECL and the CV signals of Eu_2O_3 NP/ $\text{Ru}(\text{bpy})_3^{2+}$ /GCE electrode upon changing the scan rate a 5×10^{-8} mol L^{-1} clindamycin solution was used and the results (Fig. 6b) indicated that increasing the scan rate in the range of 50 to 100 mV/s enhanced the ECL intensity with the highest signal observed at 100 mV/s. The lower intensity at lower scan rates, could be attributed to the lower formation rate for the intermediate, while this behaviour at the higher rates, is attributed to the shorter reaction time available, which leads to lower available concentrations and smaller transmission of the reaction.

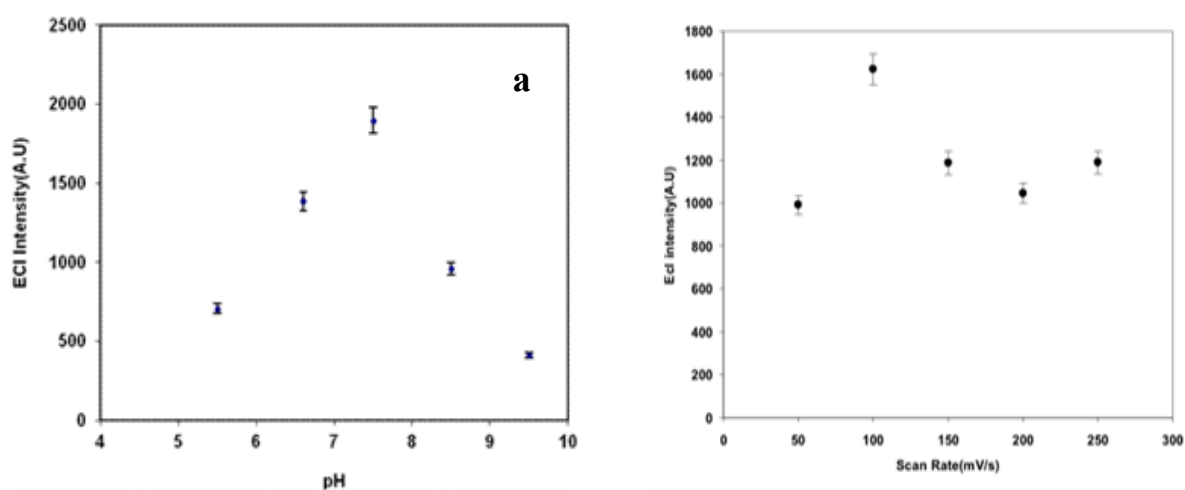


Fig. 6. (a) Effect of pH on the ECL intensity, (b) Effect of scan rate on the ECL responses of Eu_2O_3 NPs- $\text{Ru}(\text{bpy})_3^{2+}$ -GCE in 0.1 mol L^{-1} pH 7.5 phosphate buffer at 50, 100, 150, 200, and 250 mV s^{-1}

3.6. Evaluation of the interference of other species

To evaluate the selectivity of the sensor, its response profiles in 1.0 mol L^{-1} clindamycin solutions further containing common interfering species e.g. starch, talc, magnesium stearate and lactose monohydrate, which are usually present in pharmaceutical formulations, were recorded. The results did not indicate any considerable interference from the tested species.

3.7. Analytical performance

The ECL sensor was used to analyze clindamycin under optimal conditions and the signal intensity was found to be directly proportional with the clindamycin concentrations from 3.0

$\times 10^{-14}$ to 1.0×10^{-6} mol L⁻¹, and the calibration curve had a regression equation of $I = 303.63 \log C + 4289.6$ with a correlation coefficient of 0.9909 (I being the ECL response and C the concentration of clindamycin) (Fig. 7). The limit of detection of the sensor was determined to be 7.4×10^{-15} mol L⁻¹ (S/N=3).

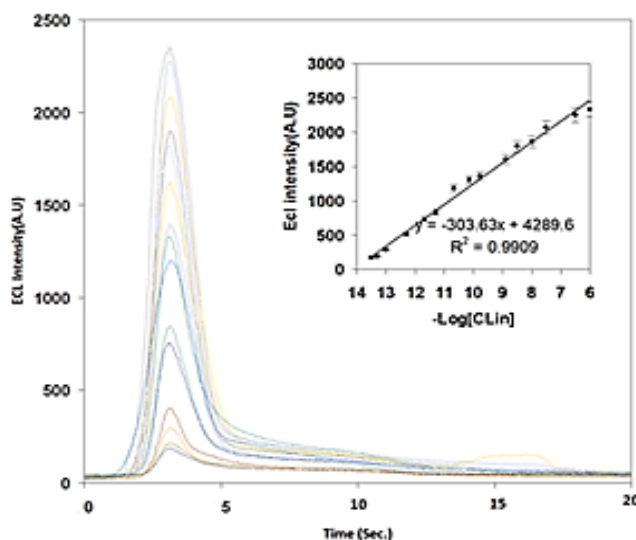


Fig. 7. ECL responses of Eu_2O_3 NPs- $\text{Ru}(\text{bpy})_3^{2+}$ -GCE at in the presence of different concentrations of clindamycin, Inset shows linear relationship between the ECL intensity and the concentration of clindamycin

Table 1. Comparisons of other reported techniques for clindamycin detection

Analytical Methods	Linear dynamic range (mol L ⁻¹)	LOD (mol L ⁻¹)	Ref.
Square-wave voltammetry	9.5×10^{-7} - 1.4×10^{-4}	2.9×10^{-7}	[2]
Differential pulse voltammetry	1.70×10^{-7} - 1.02×10^{-6}	8.61×10^{-8}	[9]
Square-wave voltammetry	3.40×10^{-7} - 2.04×10^{-6}	1.64×10^{-7}	[9]
CE with electrochemiluminescence	5×10^{-7} - 1×10^{-4}	1.3×10^{-8}	[10]
Capillary electrophoresis with capacitively coupled contactless conductivity detection	1.41×10^{-4} - 1.13×10^{-3}	8.94×10^{-5}	[61]
Molecularly imprinted sol-gel sensor	5×10^{-7} - 8×10^{-5}	2.44×10^{-8}	[62]
Derivative spectrophotometry	1.18×10^{-4} - 2.37×10^{-3}	6.73×10^{-6}	[63]
Cyclic voltammetry (EP-EPPG)	2×10^{-7} - 1.6×10^{-5}	6×10^{-8}	[64]
Differential pulse voltammetry (EP-EPPG)	3×10^{-8} - 3.2×10^{-6}	1×10^{-8}	[65]
ECL sensor	3.0×10^{-14} - 1.0×10^{-6}	7.4×10^{-15}	This work

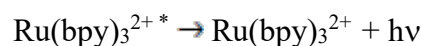
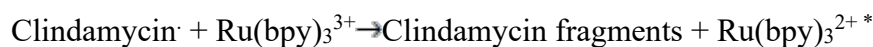
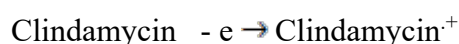
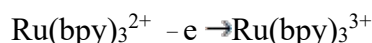
Further the analytical performance of the sensor was compared with formerly reported sensors (Table 1), and the device was found to exhibit better dynamic range and detection limit values. The reproducibility of the ECL signal produced by the sensor was further

evaluated by immersing the sensor in a PBS containing 5×10^{-8} mol L⁻¹ of clindamycin. After ten repetitive cyclic potential scans, no change was observed in the ECL intensity.

The sensor was also evaluated in terms of its stability, through the repeated ECL measurements using one sensor and after 2 months, no considerable decrease was observed in ECL response of the sensor and its response maintained about 92% of its original response, reflecting its good stability.

3.8. ECL enhancement mechanism

In the absence of clindamycin of the Eu₂O₃ NPs/Ru(bpy)₃²⁺/GCE showed a weak background ECL in the phosphate buffer, which could be attributed to the fact that the ECL emission of the system originates from the electron-transfer reaction between electrogenerated Ru(bpy)₃³⁺ and the reducing intermediate, i.e. the deprotonated form of oxidized clindamycin ion free radical, to which forms emitting excited state Ru(bpy)₃^{2+*}. This electrochemical mechanism could be considered as being analogous to the ECL mechanism reported in the case of the TPA– Ru(bpy)₃²⁺ system [26-28].



3.9. Analytical applications

Clindamycin was determined in two different pharmaceutical products. The ECL intensities observed after spiking a standard clindamycin solution into the diluted solution of samples were recorded under optimal conditions based on triplicate experiments.

Table 2. ECL determination results and recoveries of clindamycin samples using a Eu₂O₃ NPs-Ru(bpy)₃²⁺- GCE modified

Sample	Nominal value	Proposed method ^a (mg tablet ⁻¹)	Comparative method (mg)
Tablet	150	142 ±2.0	148
	300	294±5.0	298
Ampoule	150	144±3.0	149
	300	296±2.0	300

^a Average of 3 measured concentrations

The results were compared with a reference method (HPLC) and the result are summarized in Table 2. According to this data the ECL sensor offers good accuracy and repeatability and provide a great opportunity for the analysis of trace amounts of the analyte in pharmaceutical samples.

4. CONCLUSION

An ECL clindamycin sensor was prepared through modifying a glassy carbon electrode with Eu_2O_3 nanoparticles. The $\text{Ru}(\text{bpy})_3^{2+}$ immobilized on the electrode showed a diffusion-controlled electrode process and a electrocatalytic effect in the oxidation of clindamycin to form an ECL emitting species. The sensor was found to have a low detection limit of $7.4 \times 10^{-15} \text{ mol L}^{-1}$ and had a linear signal concentration profile in the range of 3.0×10^{-14} to $1.0 \times 10^{-6} \text{ mol L}^{-1}$ and its applicability to the determination of the analyte in pharmaceutical samples was also evaluated. The sensor was found to offer good reproducibility and sensitivity for clindamycin in different samples.

Acknowledgment

The authors thank the research Council of University of Tehran for financial support of this work.

REFERENCES

- [1] P. Kowalski, L. Konieczna, I Olędzka, A. Plenis, and T. Bączek, *Food Anal. Methods* 7 (2014) 276.
- [2] A. Wong, C. A. Razzino, T. A. Silva, and O. Fatibello-Filho, *Sens. Actuators B* 231 (2016) 183.
- [3] M. E. K. Wahba, N. El-Enany, and F. Belal, *Anal. Methods* 7 (2015) 10445.
- [4] X. Shao, X. Xie, and Z. Song, *Microchim. Acta.* 157 (2007) 159.
- [5] H. Sheikhoie, and K. Farhadi, *J. Iranian Chem. Res.* 3 (2010) 65.
- [6] M. Gros, S. Rodriguez-Mozaz, and D. Barcelo, *J. Chromatogr. A* 1292 (2013) 173.
- [7] E. Gracia-Lor, J. V. Sancho and F. Hernandez, *J. Chromatogr. A* 1218 (2011) 2264.
- [8] D. Frank, G. Montskó, I. Juricskay, B. Borsiczky, G. Cseh, B. Kocsis, T. Nagy, Á. K. Nagy, G. L. Kovács and A. Miseta, *J. Chemother.* 23 (2011) 282.
- [9] I. H. I. Habib, M. S. Rizk, and T. R. El-Aryan, *Pharm. Chem. J.* 44 (2011) 705.
- [10] Y. M. Liu, Y. M. Shi, Z. L. Liu, and L. F. Peng, *J. Separation Sci.* 33 (2010) 1305.
- [11] J. Wang, Z. Peng, J. Yang, X. Wang, and N. Yang, *Talanta* 75 (2008) 817.
- [12] W. Miao, *Chem. Rev.* 108 (2008) 2506.
- [13] F. Salehnia, M. Hosseini, and M. R. Ganjali, *Anal. Methods* 10 (2018) 508.
- [14] M. Hamtak, M. Hosseini, L. Fotouhi, and M. Aghazadeh, *Anal. Methds* 10 (2018) 5723.

- [15] A. Karimi, S. W. Husain, M. Hosseini, P. Aberoomand Azar, and M. R. Ganjali, *Sens. Actuators B* 271 (2018) 90.
- [16] L. Hu, and G. Xu, *Chem. Soc. Rev.* 39 (2010) 3275.
- [17] X. Y. Wang, A. Gao, C. C. Lu, X. W. He, and X. B. Yin, *Biosens. Bioelectron.* 48 (2013) 120.
- [18] M. Hamtak, L. Fotouhi, M. Hosseini, and M. R. Ganjali, *Anal. Lett.* 52 (2019) 633.
- [19] E. Sobhanie, F. Faridbod, M. Hosseini, and M. R. Ganjali, *Chemistry Select* 5 (2020) 5330.
- [20] N. Mirzanasiri, M. Hosseini, and H. Rashed, *Anal. Bioanal. Electrochem.* 10 (2018) 147.
- [21] F. Mesgari, S. M. Beigi, F. Salehnia, M. Hosseini, and M. R. Ganjali, *Inorg. Chem. Commun.* 106 (2019) 240.
- [22] M. Hosseini, M. R. Karimi Pur, P. Norouzi, M. R. Moghaddam, F. Faridbod, M. R. Ganjali, and J. Shamsi, *Anal. Methods* 7 (2015) 1936.
- [23] R. Y. Hwang, G. R. Xu, J. Hana, J. Y. Lee, H. N. Choi, and W. Y. Lee, *J. Electroanal. Chem.* 656 (2011) 258.
- [24] X. Tang, D. Zhao, J. He, F. Li, J. Peng, and M. Zhang, *A. Chem.* 85 (2013) 1711.
- [25] M. S. Wu, L. J. He, J. J. Xu, and H. Y. Chen, *Anal. Chem.* 86 (2014) 4559.
- [26] M. R. Pur, M. Hosseini, F. Faridbod, A. S. Dezfuli, and M. R. Ganjali, *Anal. Bioanal. Chem.* 408 (2016) 7193.
- [27] M. R. Karimi Pur, M. Hosseini, F. Faridbod, M. R. Ganjali, and S. Hosseinkhani, *Sens. Actuators B* 257 (2018) 87.
- [28] M. R. Karimi Pur, M. Hosseini, F. Faridbod, and M. R. Ganjali, *Microchim. Acta.* 184 (2017) 3529.
- [29] C. Xiong, H. Wang, Y. Yuan, Y. Chai, and R. Yuan, *Talanta* 131 (2015) 192.
- [30] M. H. Parvin, and M. H. Parvin, *Electrochem. Commun.* 13 (2011) 366.
- [31] F. Nemati, R. Zare-Dorabei, M. Hosseini, and M. R. Ganjali, *Sens. Actuators B* 255 (2018) 2078.
- [32] H. O. Othman, F. Salehnia, M. Hosseini, R. Hassan, A. Faizullah, and M. R. Ganjali, *Microchem.* 157 (2020) 104966.
- [33] M. Hassannezhad, M. Hosseini, M. R. Ganjali, and M. Arvand, *Anal. Methods* 11 (2019) 2064.
- [34] F. Nemati, M. Hosseini, R. Zare-Dorabei, F. Salehnia, and M. R. Ganjali, *Sens. Actuators B* 273 (2018) 25.
- [35] Z. Dehghani, J. Mohammadnejad, M. Hosseini, B. Bakhshi, and A. H. Rezayan, *Food Chem.* 309 (2020) 125690.
- [36] F. Salehnia, N. Fakhri, M. Hosseini, and M. R. Ganjali, *Application of Graphene Materials in Molecular Diagnostics, Handbook of Graphene Set* (2019).

- [37] F. Salehnia, M. Hosseini, and M. R. Ganjali, *Microchim. Acta.* 184 (2017) 2157.
- [38] K. Movlaee, M. R. Ganjali, M. Aghazadeh, H. Beitollahi, M. Hosseini, S. Shahabi, and P. Norouzi, *Int. J. Electrochem. Sci.* 12 (2017) 305.
- [39] R. M. Penner, and C. R. Martin, *Anal. Chem.* 59 (1987) 2625.
- [40] F. Mesgari, S. M. Beigi, N. Fakhri, M. Hosseini, M. Aghazadeh, and M. R. Ganjali, *Microchem. Acta* 157 (2020) 104991.
- [41] M. Hassannezhad, M. Hosseini, M. R. Ganjali, and M. Arvand, *Chemistry Select* 4 (2019) 7616.
- [42] N. Fakhri, F. Salehnia, S. Mohammad Beigi, S. Aghabalazadeh, M. Hosseini, and M. R. Ganjali, *Microchim. Acta* 186 (2019) 385.
- [43] Y. S. Borghei, M. Hosseini, M. Khoobi, and M. R. Ganjali, *J. Fluorescence* 27 (2017) 529.
- [44] M. Hosseini, M. Aghazadeh, and M. R. Ganjali, *New J. Chem.* 41 (2017) 12678.
- [45] M. R. Ganjali, P. Norouzi, A. Atrian, F. Faridbod, S. Meghdadi, and M. Giah, *Mater. Sci. Eng. C* 29 (2009) 205.
- [46] M. R. Ganjali, L. Naji, T. Poursaberi, M. Shamsipur, and S. Haghgoo, *Anal. Chim. Acta* 475 (2003) 59.
- [47] M. R. Ganjali, M. Rahimi, B. Maddah, A. Moghimi, and S. Borhany, *Anal. Sci.* 20 (2004) 1427.
- [48] M. R. Ganjali, Z. Memari, F. Faridbod, R. Dinarvand, and P. Norouzi, *Electroanalysis* 20 (2008) 2663.
- [49] M. R. Ganjali, S. Rasoolipour, M. Rezapour, P. Norouzi, A. Tajarodi, and Y. Hanifehpour, *Electroanalysis* 17 (2005) 1534.
- [50] C. Constantinescu, V. Ion, A. C. Galca, and M. Dinescu, *Thin Solid Films* 520 (2012) 6393.
- [51] K. A. Gschneidner Jr, L. Eyring, Preface, in *Handbook on the Physics and Chemistry of Rare Earths.* Elsevier (1997).
- [52] H. Mohammad Shiri, and A. Ehsani, *J. Coll. Interf. Sci.* 473 (2016) 126.
- [53] C. H. Zeng, K. Zheng, K. L. Lou, X.T. Meng, Z. Q. Yan, Z. N. Ye, R. R. Su, and S. Zhong, *Electrochim. Acta* 165 (2015) 396.
- [54] T. Anh, P. Benalloul, C. Barthou, L. thiKieu Giang, N. Vu, and L. Quoc Minh, *J. Nanomater.* 2007 (2007) 1.
- [55] N. Du, N. Du, H. Zhang, B. Chen, J. Wu, D. Li, and D. Yang, *Nanotechnology* 18 (2007) 065605.
- [56] L. Lu, X. Zhang, Z. Bai, X. Wang, X. Mi, and Q. Liu, *Advanced Powder Technol.* 17 (2006)181.
- [57] S. Lu, J. Zhang, and J. Zhang, *J. Nanosci. Nanotechnol.* 10 (2010) 2152.

- [58] A. S. Dezfuli, M. R. Ganjali, P. Norouzi, and F. Faridbod, *J. Mater. Chem. B* 3 (2015) 2362.
- [59] M. Sedaghat, P. Norouzi, and J. Shamsi, *Anal. Bioanal. Electrochem.* 6 (2014) 43.
- [60] A. W. Xu, Y. Gao, and H. Q. Liu, *J. Catalysis.* 207 (2002) 151.
- [61] P. Paul, T. Duchateau, C. Sanger-van de Griend, E. Adams, and A. Van Schepdael, *J. Separat. Sci.* 40 (2017) 3535.
- [62] Z. Zhang, Y. Hu, H. Zhang, and S. Yao, *J. Coll. Interf. Sci.* 344 (2010) 158.
- [63] M. B. Tehrani, M. Namadchian, S. Fadaye Vatan, and E. Souri, *J. Pharma. Sci.* 21 (2013) 29.
- [64] M. Hadi, and E. Honarmand, *Russian J. Electrochem.* 53 (2017) 380.
- [65] J. K. Leland, and M. J. Powell, *J. Electrochem. Soc.* 137 (1990) 3127.